Clim. Past Discuss., doi:10.5194/cp-2016-114, 2016
Manuscript under review for journal Clim. Past
Published: 21 November 2016
© Author(s) 2016. CC-BY 3.0 License.

Tropical forcing of increased Southern Ocean climate variability revealed by a 140-year subantarctic temperature reconstruction

Chris S.M. Turney[1,2*], Christopher J. Fogwill[1,2], Jonathan G. Palmer[1,2], Erik van Sebille[3,4], Zoë Thomas[1,2], Matt McGlone[5], Sarah Richardson[5], Janet M. Wilmshurst[5,6], Pavla Fenwick[7], Violette Zunz[8,9], Hugues Goosse[8], Kerry-Jayne Wilson[10], Lionel Carter[11], Mathew Lipson[1,3], Richard T. Jones[12], Melanie Harsch[13], Graeme Clark[14], Ezequiel Marzinelli[14,15], Tracey Rogers[14], Eleanor Rainsley[16], Laura Ciasto[17], Stephanie Waterman[1,3,18], Elizabeth R. Thomas[19] and Martin Visbeck[20].

[1]Climate Change Research Centre, School of Biological, Earth and Environmental Sciences, University of New South Wales, Australia
[2]Palaeontology, Geobiology and Earth Archives Research Centre, School of Biological, Earth and Environmental Sciences, University of New South Wales, Australia
[3]ARC Centre of Excellence for Climate System Science, University of New South Wales, Australia
[4]Grantham Institute and Department of Physics, Imperial College London, UK
[5]Landcare Research, PO Box 69040, Lincoln 7640, New Zealand
[6]School of Environment, University of Auckland, New Zealand
[7]Gondwana Tree-Ring Laboratory, P.O. Box 14, Little River, Canterbury 7546, New Zealand
[8]Université catholique de Louvain, Earth and Life Institute, Georges Lemaître Centre for Earth and Climate Research, Place Pasteur, 3, 1348 Louvain-la-Neuve, Belgium
[9]Earth System Science and Departement Geografie, Vrije Universiteit Brussels, Belgium
[10]West Coast Penguin Trust, P.O. Box 70, Charleston 7865, West Coast, New Zealand
[11]Antarctic Research Centre, University of Victoria, Wellington, New Zealand
[12]Department of Geography, Exeter University, Devon, EX4 4RJ, UK
[13]Department of Biology, University of Washington, Seattle, Washington, USA
[14]Evolution and Ecology Research Centre, School of Biological, Earth and Environmental Sciences, University of New South Wales, Australia
[15]Sydney Institute of Marine Science, Chowder Bay Rd, Mosman NSW 2088, Australia
[16]Wollongong Isotope Geochronology Laboratory, School of Earth and Environmental Sciences, University of Wollongong, NSW 2522, Australia
[17]Geophysical Institute, University of Bergen, and Bjerknes Centre for Climate Research, Bergen, Norway
[18]Department of Earth, Ocean and Atmospheric Sciences, University of British Columbia, Vancouver, Canada
[19]British Antarctic Survey, Cambridge, UK
[20]GEOMAR Helmholtz Centre for Ocean Research Kiel and Kiel University, Germany

Correspondence to: Chris Turney (c.turney@unsw.edu.au)

Clim. Past Discuss., doi:10.5194/cp-2016-114, 2016
Manuscript under review for journal Clim. Past
Published: 21 November 2016
© Author(s) 2016. CC-BY 3.0 License.

Abstract. Occupying 14% of the world's surface, the Southern Ocean plays a fundamental role in global climate, ocean circulation, carbon cycling and Antarctic ice-sheet stability. Unfortunately, high interannual variability and a dearth of instrumental observations before the 1950s limits our understanding of how marine-atmosphere-ice domains interact on multi-decadal timescales and the impact of anthropogenic forcing. Here we integrate climate-sensitive tree growth with ocean and atmospheric observations on southwest Pacific subantarctic islands that lie at the boundary of polar and subtropical climates (52-54˚S). Our annually-resolved temperature reconstruction captures regional change since the 1870s and demonstrates a significant increase in variability from the mid-twentieth century, a phenomenon predating the observational record. Climate reanalysis and modelling shows a parallel change in tropical Pacific sea surface temperatures that generate an atmospheric Rossby wave train which propagates across a large part of the Southern Hemisphere during the austral spring and summer.

1 Introduction

Observations during the second half of the twentieth century suggest significant but spatially complex variability in atmospheric and ocean temperature and circulation, as well as ice-sheet dynamics, across the mid- to high-latitudes of the Southern Hemisphere (Jones et al., 2016) (Figs. 1 and S1). These factors include an intensification of western boundary currents (Wu et al., 2012), a strengthening and poleward shift in the summer westerly winds associated with a positive trend in the Southern Annular Mode (SAM) (Abram et al., 2014; Marshall, 2003; Thompson et al., 2011), winter-spring warming over West Antarctica (Steig et al., 2009), latitudinal shifts in the Subantarctic and Polar fronts associated with the Antarctic Circumpolar Current (ACC) (Langlais et al., 2015), and Antarctic ice-sheet mass loss (Pritchard et al., 2012). Unfortunately, major uncertainties exist regarding their trends and interaction(s) due to high interannual variability (Fogt et al., 2012; Turner et al., 2016) and limited instrumental records prior to the 1950s (Goosse and Zunz, 2014). As a result, analysis has relied on modelling studies to infer multi-decadal to centennial variability (Freitas et al., 2015; Wang and Dommenget, 2015) and explore regional and global teleconnections (Goosse and Zunz, 2014; Langlais et al., 2015), both of which may have changed with anthropogenic forcing. This uncertainty is particularly acute in the south Pacific Ocean and adjoining regions because of the expression of central tropical ocean-atmospheric interactions associated with the El Niño-Southern Oscillation (ENSO) (Abram et al., 2014; Ciasto and Thompson, 2008; Ding et al., 2012; Schneider et al., 2012; Turney et al., 2016).

Late twentieth century Southern Ocean climate is characterised by high inter-annual variability (Jones et al., 2016; Turner et al., 2016), driven mainly by changes in the strength and location of mid-latitude westerly airflow (Thompson et al., 2011). As large-scale modes of climate variability, SAM and ENSO play a dominant role (Ciasto and Thompson, 2008; Fogt et al., 2012). Of particular significance, the positive post-1960s trend in the mid-to-high latitude pressure gradient described by SAM reaches its maximum during the austral summer (Jones et al., 2016), marked by a zonally asymmetric poleward displacement of the jet stream and strengthening of the prevailing surface westerly air flow centred on 50°S (Marshall, 2003; Thompson et al., 2011) (Fig. S2). In contrast, ENSO is associated with spatially different temperature and wind trends across mid to high latitudes (Ciasto and Thompson, 2008) (Fig. S3), with atmospheric pressure anomalies experiencing their greatest

Clim. Past Discuss., doi:10.5194/cp-2016-114, 2016
Manuscript under review for journal Clim. Past
Published: 21 November 2016
© Author(s) 2016. CC-BY 3.0 License.

Climate of the Past Discussions

amplitude during austral spring and summer in the south Pacific (Fig. S4). The pattern resembles a zonally asymmetric wave train of atmospheric pressure anomalies extending from New Zealand to the west Antarctic coast, and into the Weddell Sea–South Atlantic (the so-called Pacific-South American or PSA mode) (Mo and Higgins, 1998; Trenberth et al., 1998; Trenberth et al., 2014) (Fig. S4). The PSA has been shown to introduce zonal asymmetries in the seasonal SAM structure in the south Pacific (Fogt et al., 2012). Overall, the poleward migration of storm tracks reduces air-to-sea heat fluxes through increased cloud cover and evaporative heat loss from the ocean (Ciasto and Thompson, 2008; Thompson et al., 2011), while increasing oceanic Ekman transport of cool surface water (Ciasto and Thompson, 2008) and a competing poleward eddy heat flux (Sallée et al., 2012). As a result, sector-specific poleward shifts in westerly airflow have led to contrasting late twentieth century ocean-atmospheric trends. How the above modes of variability influenced Southern Ocean climate and ocean dynamics before the period of satellite observations remains highly uncertain (Jones et al., 2016). An improved network of quantified climate-sensitive proxy records across the mid- to high-latitudes is crucial for exploring climate teleconnections through time (Abram et al., 2014; Jones et al., 2016; Turney et al., 2015; Turney et al., 2016).

The subantarctic islands of the southwest Pacific lie at hemispherically important atmospheric and ocean boundaries, offering considerable potential for understanding long-term climate trends and the role (if any) of tropical forcing on high latitude change. Campbell (52.54˚S 169.14˚E) and Macquarie (54.50˚S 158.95˚E) islands are located just north of the main front of the ACC and south of the Subtropical Front (also known as the Subtropical Frontal Zone or Convergence) (Fig. S5) (Sokolov and Rintoul, 2009; Streten, 1988) in the core latitude of Southern Hemisphere westerly airflow (Streten, 1988), and are highly sensitive to Rossby wave propagation from the tropics to the high-latitudes (Fig. S4). Campbell and Macquarie islands have some of the longest, near-complete, continuous instrumental records in the Southern Ocean (commencing 1941 and 1948 respectively) (Table S1) supplemented by daily atmospheric and sea surface temperature (SST) measurements made at Macquarie Island between CE 1912 and 1915 as part of Sir Douglas Mawson's landmark Australasian Antarctic Expedition (AAE) (Kidson, 1946). Mawson's observations span four years and resolve the seasonal cycle, therefore allowing comparison to the continuous instrumental record from the 1940s to present day (hereafter 'the modern record'). The time series of observed temperatures on the two islands are highly correlated in the modern record (detrended July-June correlation 0.801, $p < 0.0001$), demonstrating a comparable climate regime. As a result of anomalies in the overlying wind, the surrounding waters are strongly influenced by variations in northward Ekman transport of cold fresh subantarctic surface water and anomalous fluxes of sensible and latent heat at the atmosphere–ocean interface. This has produced a cooling trend since 1979 (Figs. 1 and S1) (Ciasto and Thompson, 2008; Thompson et al., 2011), making the islands ideally placed to detect wind-driven changes in the north-south SST gradient over time.

Here we extend the instrumental record by exploiting the climate sensitivity of the southernmost growing trees in the subantarctic southwest Pacific to produce the first annually-resolved quantified temperature reconstruction for the region back to CE 1870. The maritime climates of Campbell and Macquarie islands provide a reconstruction of air and sea temperatures that demonstrates increasing variance since modern records commenced in the ~1940s. We investigate this time series with climate reanalysis and a three-dimensional

Clim. Past Discuss., doi:10.5194/cp-2016-114, 2016
Manuscript under review for journal Clim. Past
Published: 21 November 2016
© Author(s) 2016. CC-BY 3.0 License.

Earth-system model of intermediate complexity and identify the tropical Pacific sea surface temperatures as the principal driver of the observed variance, propagated by atmospheric Rossby waves during the austral spring and summer. Climate-sensitive records across the circum-Pacific demonstrate comparable trends, suggesting that tropical climate changes have been increasingly projected onto the mid to high latitudes. Subantarctic islands across the wider Southern Ocean provide crucially situated landmasses from which proxy data can be generated to test hypotheses about past and future global climate teleconnections.

2 Methods

2.1 Subantarctic island climate datasets (Macquarie and Campbell Islands)

The Australasian Antarctic Expedition (AAE) 1912-1915 atmospheric observations were taken from the isthmus at the northern end of Macquarie Island (Newman, 1929), in the same immediate area as the current Australian Antarctic Division Meteorological Station, established in late 1948 (54.50˚S 158.95˚E). The daily and monthly meteorological data from Macquarie Island was obtained from the published AAE reports (Newman, 1929) and the Bureau of Meteorology (http://www.bom.gov.au/climate/data-services/). Twice-daily SST measurements were also taken from Buckles Bay to the south east, with subsequent observations made again during the 1950s and 1960s (Loewe, 1968, 1957); unfortunately no direct measurements exist between 1916-1950. The next available continuous SST observations that can be compared to the 1912-1915 record are remote MODIS satellite measurements providing 4 km-resolved 11 μm daytime observations since 2001 (data accessed via http://gdata1.sci.gsfc.nasa.gov/); other satellite products do not resolve a spatial scale that allows a direct comparison to the localised measurements made at Macquarie Island. Although the satellite data are from a larger area than the AAE observations, the expedition vessel the S.Y. *Aurora* made SST measurements across Buckles Bay and demonstrated similar absolute values as those observed inshore, providing confidence that the comparisons are robust (Kidson, 1946). A meteorological station has operated in Perseverance Harbour, Campbell Island (52.54˚S 169.14˚E), since 1941. The dataset used here was obtained from the New Zealand National Climate Database (http://cliflo.niwa.co.nz/). Near complete instrumental records have been maintained on Campbell and Macquarie islands since observations began with no complete months missing from any of the datasets (Table S1).

2.2 Meteorological observations

To extend the satellite observations, we focused on the subantarctic Macquarie and Campbell islands in the southwest Pacific. For comparison to the AAE 1912-1915 record, modern-day atmosphere-ocean Macquarie Island measurements were compared in four-year bins (Tables S2 and S3). The interannual variability in the most complete dataset (that from Macquarie Island) is relatively large. Student's t-tests (two-tailed) of the monthly data here within each four-year average period relative to 1912-1915 indicate that the most consistently warmer conditions are during months in the austral summer (Tables S2 and S3). While we are aware of the issues surrounding multiple-testing this analysis illustrates the trend through time rather than interpreting specific comparisons.

© Author(s) 2016. CC-BY 3.0 License.

2.3 Tree-ring reconstruction (dendrochronology)

To develop the tree-ring chronology from the small trees of *Dracophyllum longifolium* and *D. scoparium* (and hybrids), a series of samples were collected from Campbell Island during 2013 as part of the Australasian Antarctic Expedition 2013-2014, and during further fieldwork in late 2014. After crossdating and measuring, the 30 tree-series were standardised to remove biological trends using the RCSigFree program (www.ldeo.columbia.edu/tree-ring-laboratory/resources/software). Within the program, various options are available for the conversion of the annual ring-width measurements into indices and we adopted the use of a more flexible regression model, the Friedman's Super Smoother (Friedman, 1984), to remove the growth trends. The ring-width measurements were first power transformed and then subtracted from the regression model to produce indices and avoid possible outlier bias (Cook and Peters, 1997). Following this, the signal-free method was applied to minimise trend distortion and end-effect biases in the final chronology (Fig. 2) (Melvin and Briffa, 2008). Comparison between the detrended series and average raw measurements (Fig. 2) demonstrate the standardisation process (or any of the other models) made the series heteroscedastic. The relationship of the tree-ring chronology to the Campbell and Macquarie Islands temperature records and Southern Annular Mode (SAM) reconstruction (Visbeck, 2009) was explored using bootstrapped correlation function analysis in the bootRes R software package (Figs. 2 and S16) (Zang and Biondi, 2012). bootRes uses 1000 bootstrapped samples to compute Pearson's correlation coefficients between the tree-ring parameter and each of the climatic predictors and then to test their significance at the 0.05 level. Bootstrap samples are drawn at random with replacement from the selected time interval. Median correlation coefficients are deemed significant if they exceed, in absolute value, half the difference between the 97.5th quantile and the 2.5th quantile of the 1000 estimates (Biondi and Waikul, 2003). In the plots the darker bars indicate a coefficient significant at $p < 0.05$ and the lines represent the 95%-confidence interval.

Based on these results, the Campbell Island "growing-season" of monthly temperatures from October to March (six months, spanning from spring to autumn) was selected for reconstruction using the *Dracophyllum* chronology for the period 1870-2013 (Expressed Population Signal or EPS>0.85). Similarly for Macquarie Island, the same growing season was selected (October-March; six months). For SAM, we find the most significant relationship was for July-October. The program PCReg (www.ldeo.columbia.edu/tree-ring-laboratory/resources/software) was used to carry out a linear regression model of the tree-ring chronology to the selected growing-season windows for both Campbell and Macquarie Islands. A split-period for calibration/verification analysis was used (Cook and Kairiukstis, 1990) to test the regression model robustness. Two rigorous tests of the regression models performance, the reduction of error (RE) and the coefficient of efficiency (CE) were calculated (Table S4). Our model for Campbell Island passed both the CE and RE tests (i.e. positive) indicating that the model was skillful in reconstructing observed variations, however the verification results for Macquarie Island were weaker and just failed for the more rigorous CE test. We then used the full period of instrumental data (1949-2012 for Campbell Island and Macquarie Island) to develop final models and reconstruct "growing-season" temperatures back to 1870 for both islands (Figure 3). The prediction intervals (90% quantile limits) associated with the reconstructed temperatures were produced using a fixed *t*-statistic for scaling the uncertainties (Olive, 2007). Importantly, the chronology is derived from a mixture of tree

Clim. Past Discuss., doi:10.5194/cp-2016-114, 2016
Manuscript under review for journal Clim. Past
Published: 21 November 2016
© Author(s) 2016. CC-BY 3.0 License.

Climate of the Past Discussions

ages (i.e. the oldest started in CE 1747 and the youngest in 1958) and is not made up of a single cohort of similar aged trees that have matured across the same period.

2.4 Spectral Analysis

To investigate climate periodicities we undertook multi-taper method (MTM) analysis on the *Dracophyllum* temperature reconstruction (Figure 4), tree chronology (Figure S9) and annual southwest Pacific SSTs (Figure S10) (the latter derived from Hadley Centre Ice and Sea Surface Temperature; HadISST) (Rayner et al., 2003) using a narrowband signal and red noise significance (with a resolution of 2 and 3 tapers) (Thomson, 1982) with the software *kSpectra* version 3.4.3 (3.4.5).

2.5 Characterising water mass sources and ocean fronts

In order to characterise the decadally-averaged source(s) of water masses near Macquarie and Campbell islands, we performed an experiment with virtual particles in an eddy-resolving ocean model (the Japanese Ocean model For the Earth Simulator or OFES) (Masumoto et al., 2004), which has a 1/10° horizontal resolution and near-global coverage between 75°S and 75°N, and has a demonstrated ability for modeling changes in the Southern Ocean between 2000 and 2010 (van Sebille et al., 2012) (Fig. S5). While OFES precludes us from modelling the warming across the 1970s, it does allow us to hindcast the origin of the waters down to a depth of 400 metres using Lagrangian analysis in the most-recent decade. Assuming a steady-state ocean circulation, this analysis allows us to refine our understanding of the sources and by association boundaries of water masses surrounding Macquarie and Campbell islands. The model was forced using NCEP wind and flux fields and output is available as three-day averages (Qin et al., 2014).

Particles were released every three days between 1 January 2005 and 31 December 2010 on a latitude-depth section at 170°E, every 0.1° in latitude between 60°S and 45°S and every 50 m in depth between 25 m and 300 m, for a total of 318,288 particles. The particles were then advected backwards in time within the three-dimensional OFES velocity fields using the fourth-order Runge-Kutta method as implemented in the Connectivity Modeling System (CMS) version 1.1b (Paris et al., 2013). The particles were advected for five years, or until they reached 30°S or 0°E. Once all the particles were integrated, they were categorised into those that start in the Agulhas Current (at 30˚S and between 28˚E and 40˚E) and those that start in the East Australian Current (at 30˚S and between 150˚E and 160˚E).

Using the western Indian Ocean boundary Agulhas Current as a tracer for the Subtropical Front (and the southern limit of the Subtropical Gyre) (Wang et al., 2014) we identify a pathway of particles flowing from the Cape of Good Hope to the southwest Pacific subantarctic islands (Fig. S5). The particles that connect to the region around Macquarie and Campbell islands follow a very narrow and almost linear path southeastward across Indian Sector of the Southern Ocean. The fastest particles reach Macquarie Island less than two years after release in the Agulhas Current, with the majority arriving between three and four years after release. In contrast, little leakage from the East Australian Current is observed, with approximately six times more Agulhas

Clim. Past Discuss., doi:10.5194/cp-2016-114, 2016
Manuscript under review for journal Clim. Past
Published: 21 November 2016
© Author(s) 2016. CC-BY 3.0 License.

particles delivered to the southwest Pacific subantarctics than the East Australian Current (EAC) (Wu et al., 2012) (Fig. S5).

2.6 Modelling transient change

General circulation models (GCMs) involved in the Fifth Coupled Model Intercomparison Project (CMIP5) (Taylor et al., 2011) struggle to simulate the observed internal variability and/or seasonal cycle over the Southern Ocean (Wang et al., 2015; Zunz and Goosse, 2015), supported by the poor correlations observed between our reconstructed and CMIP5 October-March temperatures (Table S6). Here we take an alternative approach. The 3-D Earth-system model of intermediate complexity LOVECLIM1.3 (Goosse et al., 2010) used here includes representations of the atmosphere (ECBilt2) (Opsteegh et al., 1998), the ocean and the sea ice (CLIO3) (Goosse and Fichefet, 1999), and the vegetation (VECODE) (Brovkin et al., 2002). The atmospheric component is a T21 (corresponding to a horizontal resolution of about 5.6˚ × 5.6˚), three-level quasi-geostrophic model. The oceanic component consists of an ocean general circulation model coupled to a sea-ice model with horizontal resolution of 3˚ × 3˚ and 20 unevenly spaced vertical levels in the ocean. The vegetation component simulates the evolution of trees, grasses and desert, with the same horizontal resolution as ECBilt2. The experiments analysed here cover the period CE 1850– 2009, driven by the same natural (solar and volcanic) and anthropogenic (greenhouse gas, sulfate aerosols, land use) forcings (Goosse et al., 2006) as the ones adopted in the historical simulations performed in the framework of CMIP5 (Taylor et al., 2011). The initial conditions are derived from a numerical experiment covering the years CE 1–1850 using the same forcing, in order to take into account the long memory of the Southern Ocean (Goosse and Renssen, 2005). For the CE 1850–2009 simulations, the model was forced to follow the observations of surface temperature from the HadCRUT3 dataset (Brohan et al., 2006) using a data assimilation technique based on particle filtering (Dubinkina and Goosse, 2013; Goosse et al., 2006). A simulation without additional freshwater flux (no freshwater flux) with data assimilation, from CE 1850 to 2009, was analyzed here (Zunz and Goosse, 2015), allowing direct comparison between climate parameters and SST trends across the Southern Ocean. SSTs for the Macquarie-Campbell island sector and anomalies in zonal wind stress are shown in Figures 8 and 9 respectively.

3 Results

3.1 Modern climate changes

Comparing atmospheric temperatures during the 1912-1915 AAE observational period and the modern record from Macquarie Island shows high interannual variability (Fig. 1B). Whilst the temperature trend across the period of satellite observations appears to describe a cooling trend in the southwest Pacific, significant warming is observed across the annual and spring-summer months from the 1960s and peaks during the 1980s (Figs. 1 and S6, Table S2). No parallel changes are observed in wind direction (Fig. S7) or sunshine hours (Fig. S8). The number of ocean observations are more limited but comparable (0.5˚C) warming was observed across the 1950s-1960s with MODIS satellite measurements (MODerate Imaging Spectroradiometer; 2000-2014) demonstrating slightly cooler waters during the present day (though still 0.3˚C warmer than the AAE period) (Table S3). A similar long-term trend is also observed with air and sea temperatures at Campbell Island

(Morrison et al., 2015). Importantly, because of their small size and highly maritime climate, atmospheric temperatures on the islands parallel the seasonal SST cycle (Fig. 1C), indicating a tight thermal coupling between air and sea surface temperatures (Kidson, 1946; McGlone et al., 2010; Thompson et al., 2011), providing a sensitive terrestrial measure of Southern Ocean conditions.

3.2 Extending the temperature record

To develop an annually-resolved temperature reconstruction for the southwest Pacific that will extend the modern instrumental record we sampled 30 *Dracophyllum* spp. trees on Campbell Island as part of the AAE 2013-2014 (Fig. 2). Here two *Dracophyllum* species (and hybrids) form the southernmost growing evergreen shrubs and small trees in the southwest Pacific (with no *Dracophyllum* on Macquarie Island). *Dracophyllum* spp. are known to be responsive to warmer temperatures and capable of reaching ages of >200 years (Harsch et al., 2014), providing an opportunity to derive a continuous proxy record of temperature in this key region spanning more than a century. Because of the coherent climate trends on both islands, the relationship of tree-ring growth to Campbell and Macquarie Islands temperature records was explored using bootstrapped correlation function analysis in the bootRes R software package (Zang and Biondi, 2012) to identify the monthly temperature responses, followed by a split-period for calibration/verification analysis to test the regression model robustness using the reduction of error (RE) and the coefficient of efficiency (CE) (Fig. 2 and Table S4). Based on those results, we selected an austral 'growing season' window for linear regression modelling to produce spring-summer (October-March) temperature reconstructions for Campbell and Macquarie islands.

3.3 Changing climate variability

The *Dracophyllum* reconstructions extend the surface air temperature record for the southwest Pacific sector of the Southern Ocean back to CE 1870 (Fig. 3). We find growing season (spring-summer) temperatures parallel meteorological observations on the subantarctic islands for the period of overlap (including the original AAE) (Fig. 3), with a long-term trend towards increasing temperatures from the 1960s that reached a maximum during the late 1980s (~1˚C warmer on Macquarie Island compared to period 1912-1915). Peak temperatures of the 1980s, however, were not sustained in the southwest Pacific through to present day (Fig. 1). Instead, a notable feature of our 140-year reconstruction is the long-term change in variability captured by a 30-year running standard deviation, regardless of the standardisation method used (Figs. 3C and S10). We observe a sustained increase from the ~1940s compared to intermediate levels of variance during the late nineteenth century and a minimum during the first half of the twentieth century. The high number of replicated trees across the reported series means we can discount changing sample depth as the cause of increasing variance. Removing extreme values centred on 1956, 1979 and 1986 does not substantially change the shift to higher variance in the second half of the twentieth century (Fig. S9), demonstrating that the long-term trend is robust. To test for the significance of this change, we compared the variance across the tree-ring record (CE 1870-1941 vs 1941-2012) and found the second half of the twentieth century is significantly larger for all standardization approaches (Friedman F and Bartlett's K-squared tests p = 0.0055; Table S5), suggesting a shift in climate to one characterised by pervasive high variability.

© Author(s) 2016. CC-BY 3.0 License.

To further investigate the change in temperatures across the record we undertook multi-taper method (MTM) spectral analysis on the reconstructed air temperature and associated tree-ring index (Figures 4 and S11). We find the strongest periodicities in growing season temperatures over two narrow windows, 3 and 2.4 years (all above 95% confidence), identical to those recognized in regional SSTs extracted from HadISST (Rayner et al., 2003) (Fig. S12). Hovmöller plots of satellite-observed SSTs between 45˚ and 55˚S confirm a pattern of alternating warm and cool temperatures in the southwest Pacific subantarctic islands with these periodicities (Fig. S13). Our new extended temperature series therefore indicates the late nineteenth and early twentieth century climate was characterised by low inter-annual variability with increasing amplitude in the 3 and 2.4-year bands from the ~1940s and late 1960s respectively (Figure 4B). We therefore conclude the increased amplitude of the 3 and 2.4-year bands is a robust climate feature in the southwest Pacific since the 1940s.

3.4 Marine population changes

Intriguingly, the observed increase in variance reported here appears to coincide with a regional order of magnitude decline in the populations of many marine species spanning Macquarie Island to the Antipodes Islands, including penguins and elephant seals (Morrison et al., 2015; Weimerskirch et al., 2003). Whilst not a major focus of the present study, recent work has illustrated how multi-stressors (including climate variability) can impact on Southern Ocean biota (Boyd et al., 2015) and the potentially dramatic biological responses that can result across different trophic levels (Trathan et al., 2007). The following therefore provides a brief summary of population trends for comparison to the climate and ocean trends and variability reported here.

Because of the scarcity of island breeding sites and their limited foraging range while breeding, subantarctic penguins are particularly susceptible to climate change and associated changes in marine parameters. Penguins, or other top predators, may respond to changes in food availability when marine parameters change by retracting or expanding their distributions, with changes in population size or breeding phenology (Weimerskirch et al., 2003). Alternatively, climate change can affect penguin numbers due to changes in conditions ashore. For example, at Punta Tombo in Argentina since 1960 storms have become more frequent and more intense causing the deaths of Humboldt penguin (*Spheniscus humboldti*) chicks (Boersma and Rebstock, 2014). At Punta Tombo, chick deaths due to storms were additive to deaths due to other factors. It is important to note, however, that there is usually a lag between climate change and any subsequent change in penguin (or other predator) population; the lag time depending on whether climate affects adult or chick survival, recruitment or some other demographic parameter (Weimerskirch et al., 2003).

In the New Zealand subantarctic there have been pronounced declines in the numbers of Eastern Rockhopper penguins (*Eudyptes filholi*) at Campbell Island, and both Rockhopper and Erect crested penguins (*E. sclateri*) on the Antipodes Islands (49.68˚S 178.75˚E). J.H. Sorensen estimated there were about three million Rockhopper penguins on Campbell Island in the early 1940s (Cunningham and Moors, 1994). Subsequent analysis of Sorensen's photos suggests this estimate was too high, and the 1940s breeding population has been more accurately estimated at 1.6 million birds (Cunningham and Moors, 1994). Sorensen's observations suggest that the decline began in the mid-1940s; photos show the decline continued through the 1950s followed by a brief

© Author(s) 2016. CC-BY 3.0 License.

resurgence in numbers, before a further decline that began no later than the mid-1970s (Cunningham and Moors, 1994). By 2012, Rockhopper numbers on Campbell Island had suffered a 95.5% decline (of which 94% had occurred by the mid-1980s) (Morrison et al., 2015). Allowing for a lag of several years for chicks to reach breeding age, the changes in Rockhopper penguin numbers correlate with changes in sea water temperatures recorded in Perseverance Harbour which increased to a peak between 1945 and 1950, declined between 1950 and 1965, then increased sharply by 1970 (Cunningham and Moors, 1994; Morrison et al., 2015).

For the Antipodes, data on the decline in both Eastern Rockhopper and Erect crested penguin populations cover a shorter period, but are more robust. Whole island group surveys have been conducted on three occasions and, although there were some differences in counting methodology and time of year in which counts were made, the decline in both species has been huge; in 2011 there were only about 5% as many Rockhopper penguins and fewer than half as many Erect crested penguins as there were in 1978 (Table S7) (Hiscock and Chilvers, 2014). Whilst no climate data is available from the Antipodes Islands, this subantarctic archipelago falls within the same climate zone as Macquarie and Campbell Islands (Fig. 1) and is therefore assumed to have experienced the same long-term trend in air and sea surface temperatures.

4 Discussion

Whilst the southwest Pacific subantarctic islands lie along the northern edge of the ACC and south of the Subtropical Front (Fig. S5), the absence of propagating SST signals across the Southern Ocean suggests that movement of ocean boundaries and/or changing input of marine western boundary currents (Figs. S5 and S13) are not primary drivers of the observed increased variability. An alternative scenario for the increasing amplitude in the 3 and 2.4-year bands is a change in atmospheric circulation. To identify a possible atmospheric mechanism, we compared air temperatures over Macquarie Island with estimates from ERA Interim reanalysis (Dee et al., 2011) and observe a significant positive correlation to spring-summer atmospheric pressure anomalies (deseasonalised and detrended at 850 hPa) since 1979 (Fig. 5A) and inverse relationships with temperature and zonal and meridional wind stress (Figs. 5B and S14). Cooler temperatures over Macquarie Island are therefore associated with a centre of relatively low pressure (at 850 hPa) south of New Zealand and enhanced westerly and southerly airflow across a broad longitudinal band spanning 120˚ to 150˚E (significance $p_{field} < 0.05$). A similar significant positive correlation to spring-summer SSTs is also observed (Fig. 5C), supporting our earlier observation of the thermal coupling between atmospheric and ocean temperatures but extending across the broader southwest Pacific. Although we find no evidence for a long-term shift in airflow direction or solar radiation that parallel the observed trend in subantarctic temperatures (Figs. S7 and S8) we do observe a marked change in wind strength since the original AAE of 1912-1915, with a long-term intensification (but higher variability) of winds over Macquarie Island (Fig. 5D). Our results are consistent with the observed (post-1979) spring-summer trend towards windier conditions in the southwest Pacific (Fig. S1).

Whilst some studies have suggested a dynamical atmospheric circulation response to ozone layer depletion over the Southern Hemisphere mid-latitudes since the 1990s (Thompson et al., 2011), the reconstructed 2.4 and 3-year periodicities suggest a tropical teleconnection with the southwest Pacific (Adamson et al., 1988; Kestin et

Clim. Past Discuss., doi:10.5194/cp-2016-114, 2016
Manuscript under review for journal Clim. Past
Published: 21 November 2016
© Author(s) 2016. CC-BY 3.0 License.

al., 1998). Using the HadISST (Rayner et al., 2003) and ERA Interim (Dee et al., 2011) datasets, a significant inverse correlation is observed between subantarctic and central-eastern low latitude Pacific temperatures and zonal wind stress, with a relatively warm (cool) eastern equator associated with weaker (stronger) mid-latitude westerly winds and cooler (warmer) SSTs in the southwest Pacific (Figs. 5A-C). Comparison to different measures of tropical Pacific SSTs and atmospheric circulation indicate the most significant relationship with subantarctic spring-summer temperatures is the Nino 3 region (correlation -0.592, $p < 0.001$) (Table 1).

To elucidate the mechanism by which changes in the tropical Pacific may be projected onto the high latitudes, we explored the relationship between Nino 3 temperatures and Southern Hemisphere atmospheric circulation using data from ERA Interim (Dee et al., 2011) (Fig. 6). We observe a Rossby wave train similar to the PSA climate mode of variability during the austral spring-summer (Ding et al., 2012; Mo and Higgins, 1998; Trenberth et al., 1998). We find that post-1979, warmer temperatures in the Nino 3 region leads to deep convection and upper-level divergence flow (at 300 hPa) (Ding et al., 2012; Fogt et al., 2012; Trenberth et al., 1998) (Fig. S15), forcing an atmospheric Rossby wave train southeast into the extratropics manifested as cyclonic anomalies south of New Zealand – consistent with the relationship observed with Macquarie Island temperatures (Fig. 5) – that extend across the Pacific as anticyclonic anomalies in the Amundsen-Bellingshausen seas and cyclonic anomalies off the east coast of South America (Ciasto and Thompson, 2008; Mo and Higgins, 1998). Lead-lag analysis demonstrates the atmospheric signal propagates over southern New Zealand during the late austral winter and reaches the Amundsen-Bellingshausen seas by the summer (Fig. S16). Our results support previous studies that find the PSA signal precedes peak temperatures by approximately one season and abruptly weakens during the austral summer (Schneider et al., 2012) (Figs. S4 and S16).

With the above tropospheric pressure changes (Fig. 6) we suggest warmer Nino 3 temperatures are associated with stronger westerly airflow over the southwest Pacific subantarctic islands and west Antarctic coast, accompanied by enhanced southerly airflow across the Antarctic Peninsula that extends into the south Atlantic. Hovmöller plots show an alternating pattern of warm-cold surface temperatures between the southwest Pacific and Amundsen-Bellingshausen seas using both the HadISST (Rayner et al., 2003) and Reynolds v2 SST (Smith and Reynolds, 2005) datasets (Fig. S13), consistent with atmospheric Rossby wave propagation and regional ocean surface responses. Running 30-year correlations between the *Dracophyllum* series and measures of westerly airflow, however, suggests no relationship with a hemispheric-wide reconstruction of SAM that extends back to CE 1884 (Fig. 7A) (Marshall, 2003; Visbeck, 2009). Regional monthly changes in the structure of SAM are now recognized and allow sector-specific analysis (Ding et al., 2012; Fogt et al., 2012; Visbeck, 2009). Here we identify a significant inverse correlation to the Australasian region for the austral winter and spring during the post 1940s period ($p < 0.05$; Fig. 7C), while the Southern Hemisphere-wide and regional South American and African SAM reconstructions do not appear to be significant for any period across the twentieth century (Figs. 7B and C). Previous work has demonstrated that the PSA is an important contributor to the zonal asymmetry in SAM (Ding et al., 2012; Fogt et al., 2012), suggesting the tropics are indeed imposing a signal on mid-latitude westerly airflow in the southwest Pacific. However, in contrast to earlier studies that have postulated anthropogenic forcing may have changed the structure of SAM to be more zonal (Fogt et al., 2012),

Clim. Past Discuss., doi:10.5194/cp-2016-114, 2016
Manuscript under review for journal Clim. Past
Published: 21 November 2016
© Author(s) 2016. CC-BY 3.0 License.

our results imply the tropics have introduced an asymmetry to the Australasian sector of SAM in the modern record, or this has at least become more common during the second half of the twentieth century.

To investigate whether the changes in the southwest Pacific subantarctic region are representative of a larger part of the Southern Hemisphere we analysed simulations with the three-dimensional Earth-system model of intermediate complexity LOVECLIM1.3 for CE 1850– 2009, driven by natural (solar and volcanic) and anthropogenic (greenhouse gases, sulphate aerosols, land use) forcings (Zunz and Goosse, 2015) (Fig. 8). For the 1850–2009 simulation, the model was forced to follow the observations of surface temperature. We examined the changes in zonal wind stress between selected decades across the twentieth century, including 1910-1919 (overlapping the original AAE period) (Fig. 8). Over the past century, we find increasingly stronger westerly winds across the Southern Ocean with a marked intensification in the southwest Pacific and Antarctic Peninsula during the most recent decades with more easterly airflow over the Ross Sea (Fig. 8C), trends also observed in estimates derived from the ERA Interim dataset (Dee et al., 2011) and the modern Macquarie Island record (Figs. 5D and 8D).

Although there appears to have been a long-term strengthening of westerly winds across key sectors of the mid-latitudes, the Macquarie Island record suggests this has also been accompanied by increasing variability (Fig. 5D). To explore whether this is manifested across the wider Pacific we compared our 140-year temperature reconstruction to key datasets (Fig. 9). We observe parallel changes in SST magnitude and trend in the southwest Pacific using both the LOVECLIM model output and HadISST (Rayner et al., 2003) (Figs. 3 and 9D), consistent with subantarctic island temperatures. The close similarity between the LOVECLIM output and HadISST argues against any bias in the latter dataset for this region (Chelton and Risien, 2016). Intriguingly, the inferred increasing westerly winds and warming Southern Ocean in the southwest Pacific have been accompanied by a regional order of magnitude decline in marine vertebrate populations (Morrison et al., 2015), suggesting the increased inter-annual temperature variability may have played a role, and will form a focus for future work. Importantly, we find a comparable increase in temperature and variance in the Nino 3 region, supporting our contention that the tropics are a major driver of variability across the subantarctic Pacific and implying similar variability may be expressed across other sectors of the Southern Ocean, albeit lagged by 1-3 months (Fig. S16). To test this we utilise snow core accumulation records from coastal West Antarctica, a region identified as sensitive to atmospheric pressure anomalies associated with the PSA (Thomas et al., 2008) (Fig. 6). Previous studies have reported a mid to late twentieth century increase in precipitation associated with a deepening of the Amundsen Sea Low (ASL) (Thomas et al., 2015; Thomas et al., 2008), where strong northerlies advect warm south Pacific air masses over the continent, resulting in orographic-driven precipitation over the southern Antarctic Peninsula (Gomez ice core; Fig. 9F) and the West Antarctic coastal sites Bryan Coast and Ferrigno (Fig. S17). Importantly the observed twentieth century increase appears to be confined to the Antarctic Peninsula and West Antarctic coast, with the magnitude decreasing from east (Gomez) to west (Ferrigno); in marked contrast, the observed increase is not recorded in the continental interior (Thomas et al., 2015). Whilst the ASL is generally considered quasi-stationary because of the large number of low pressure systems in this sector of the circumpolar trough (Hosking et al., 2013), the snow core derived increases in precipitation are accompanied by an increase in 30-year running mean of the standard deviation, suggesting

© Author(s) 2016. CC-BY 3.0 License.

increased variability in the ASL region that is unusual in the context of the past 300 years, with the Gomez site most sensitive to changes in synoptic conditions.

Whilst we cannot preclude that the climate teleconnections may have been different prior to the 1940s, the parallel changes in variance observed across the Pacific suggests this is not likely (Figure 9). This interpretation is supported by the recently reported stepped increase in spring-summer rainfall over the south Atlantic during the 1940s, a shift apparently unprecedented over at least the last 6000 years, and interpreted to be a consequence of highly seasonal changes in atmospheric pressure over the Amundsen-Bellingshausen seas (Turney et al., 2016). Although analysis of the most recent decade suggests a weakening of the PSA (Trenberth et al., 2014), the observed persistently high spring-summer Pacific variance and increase in Atlantic precipitation (Turney et al., 2016) suggests that Rossby wave penetration of the high latitudes remains substantial when placed in the context of the last 140 years (Figure 9).

5 Conclusions

Our study adds to a growing body of literature that increasing and variable tropical temperatures are a major driver of spring-summer Southern Hemisphere atmospheric circulation changes (Ciasto and Thompson, 2008; Jones et al., 2016; Schneider et al., 2012; Steig et al., 2009; Wang and Dommenget, 2015). Our findings, however, provide a long-term perspective that suggests modern observed high interannual variability was established across the 1940s, and that contemporary equatorial Pacific temperatures may now be a permanent feature across the mid to high latitudes. Further work is now required to extend key records and explore climate variability back through the Holocene (Cobb et al., 2013). This study emphasises the considerable value of tree ring and historical data for extending satellite observations of the Southern Ocean beyond 1979 (Goosse and Zunz, 2014), and the use of ocean and climate models to interpret trends in rapidly changing terrestrial and marine environments. Our results offer the potential to improve forecasts across the extratropical region (Trenberth et al., 1998) and have implications for the interpretation of proxy data from locations with non-stationary relationships to modes of Southern Hemisphere atmospheric circulation.

Author Contribution

CT and CF conceived the research; CT, JP, EvS, ZT, SR, PV, VZ, HG, K.-J.W. designed the methods and performed the analysis; CT wrote the paper with input from all authors.

Competing Interests

The authors declare that they have no conflict of interest.

Acknowledgements

A large thanks to the captain and crew of the *MV Akademik Shokalskiy*, and Henk Haazen and Kali Kahn on the *Tiama* for all their help in the field. Thanks also to Lisa Alexander (CCRC) for the analysis of meteorological

© Author(s) 2016. CC-BY 3.0 License.

datasets and to Jean-Baptiste Sallee who kindly provided the location of the main fronts of the ACC (Figure 1). This work was supported by the Australasian Antarctic Expedition 2013-2014, the Australian Research Council (FL100100195, FT120100004, DE130101336 and DP130104156) and the University of New South Wales. Research on the New Zealand subantarctic Campbell Island was undertaken under Department of Conservation National Authorisation Numbers 37687-FAU and 39761-RES.

© Author(s) 2016. CC-BY 3.0 License.

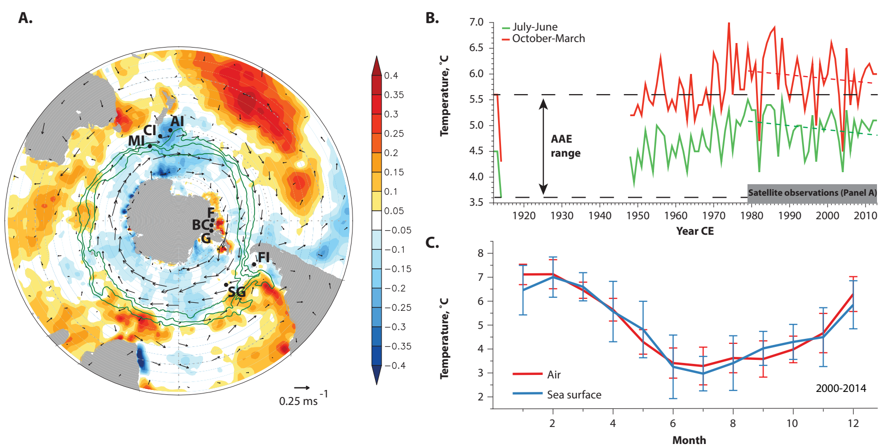

Figure 1. Twentieth century climate trends in the Southern Hemisphere. A. Austral sea surface temperature (SST; shading) and 925-hPa winds (vectors) for December-February since 1979. Key sites discussed in text are shown: Macquarie Island (MI), Campbell Island (CI), Antipodes Island (AI), Ferrigno (F), Bryan Coast (BC), Gomez (G) (Thomas et al., 2015; Thomas et al., 2008), Falkland Islands (FI) and South Georgia (GI) (Turney et al., 2016). Overlaid in green are the three main fronts of the Antarctic Circumpolar Current (Sallée et al., 2012). **B.** Annual (July-June) and spring-summer (October-March) air temperatures at Macquarie Island. Dashed lines denote range of the Australasian Antarctic Expedition temperatures (AAE; CE 1912-1915). Period of satellite observations (Panel A.) shown by grey bar; dashed coloured lines denote trend in temperatures across the satellite period. **C.** Monthly Macquarie Island air (red line) and sea surface temperatures (blue line) (with 1σ) demonstrating tight coupling between atmospheric temperature and SSTs (2000-2014).

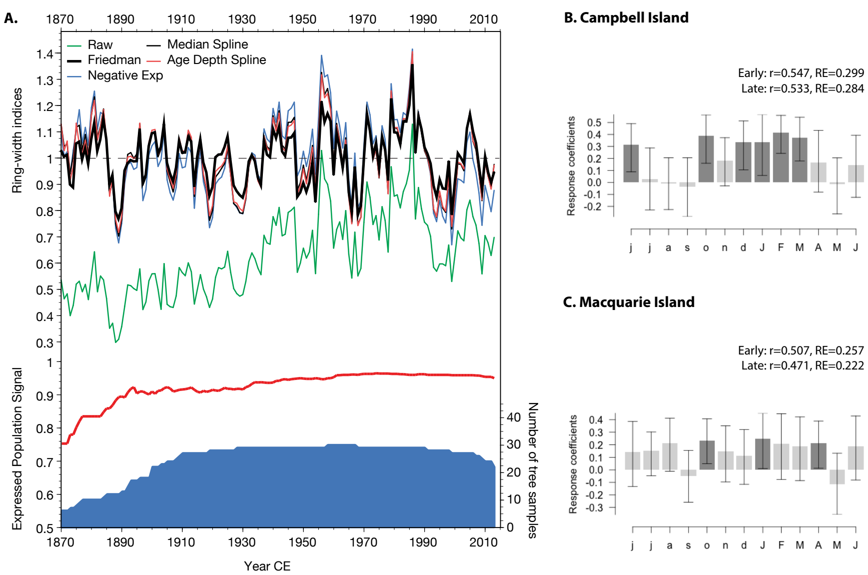

Figure 2. Developing a temperature-sensitive tree-ring record from the subantarctic Pacific. A. *Dracophyllum* raw tree-ring chronology (green line) with different standardization outputs (various coloured lines), Expressed Population Signal (EPS; thick red line) and sample size of trees (blue area). Bootstrap correlation function of the *Dracophyllum* tree-ring chronology to instrumental records of monthly temperatures from Campbell Island (**B.**) and Macquarie Island (**C.**) with error statistics for early (CE 1949-1980) and late (1981-2012) calibration periods. Darker bars indicate months with statistically significant correlations ($p < 0.05$).

© Author(s) 2016. CC-BY 3.0 License.

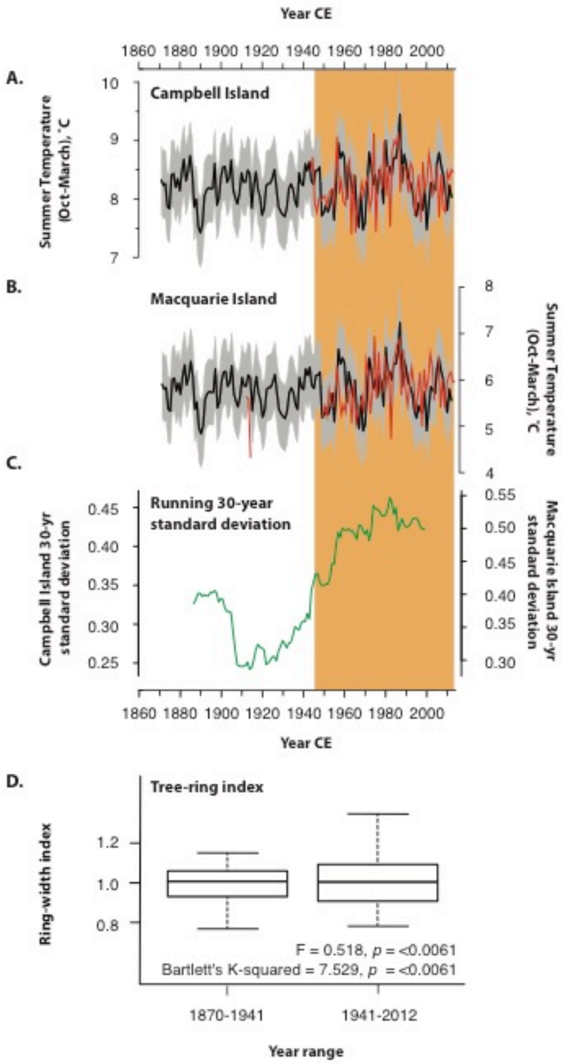

Figure 3. 140-year temperature variability in the subantarctic Pacific. Campbell Island (**A.**) and Macquarie Island (**B.**) observed (red lines) and *Dracophyllum* reconstructed (black) growing season temperatures (October-March) with 90% quantile limits (grey envelope) compared against running 30-year mean standard deviation of the reconstructed temperature series (**C.**). **D.** Box and whisker plots of the ring width indices with summary statistics indicating a significant difference in variance between the periods 1870-1941 and 1941-2012. Orange column defines significant post-1940s temperature variability in the record.

© Author(s) 2016. CC-BY 3.0 License.

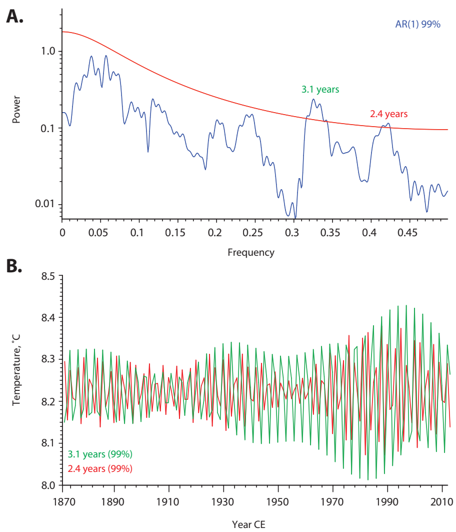

Figure 4. Tropical variability in the subantarctic temperature record. Changing amplitude of reconstructed summer temperatures for Macquarie Island. Multi-taper method (MTM) (**A.**) and extracted climate periodicities exceeding 99% significance (**B.**) observed in the *Dracophyllum*-derived growing season temperature reconstruction for Macquarie Island since CE 1870.

© Author(s) 2016. CC-BY 3.0 License.

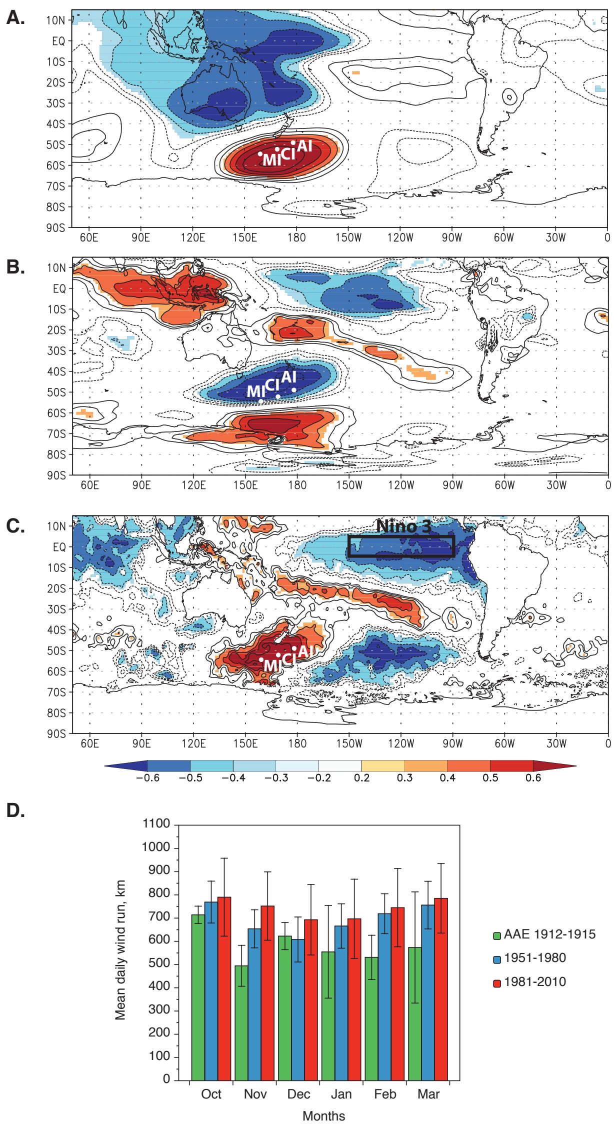

Figure 5. Climate controls on temperature over Macquarie Island. Spatial correlations between detrended and deseasonalised Macquarie Island mean monthly atmospheric temperatures (October-March) and 850 hPa height (**A.**), zonal wind stress using ERA Interim[31] (**B.**) and sea surface temperature (HadISST; **C.**) (Rayner et al., 2003) for the period 1979-2013. Note: Campbell Island (CI) and the Antipodes Islands (AI) fall within the region of greatest correlation to SSTs in the southwest Pacific. Nino 3 region also shown. Significance $p_{field} < 0.05$. For comparison, mean daily wind run (kilometres) at Macquarie Island for October-March from the Australasian Antarctic Expedition (1912-1915) and 30-year periods (1951-1980 and 1981-2010) with 1σ uncertainty (source: Bureau of Meteorology) (**D.**).

Clim. Past Discuss., doi:10.5194/cp-2016-114, 2016
Manuscript under review for journal Clim. Past
Published: 21 November 2016
© Author(s) 2016. CC-BY 3.0 License.
Climate of the Past Discussions
Open Access

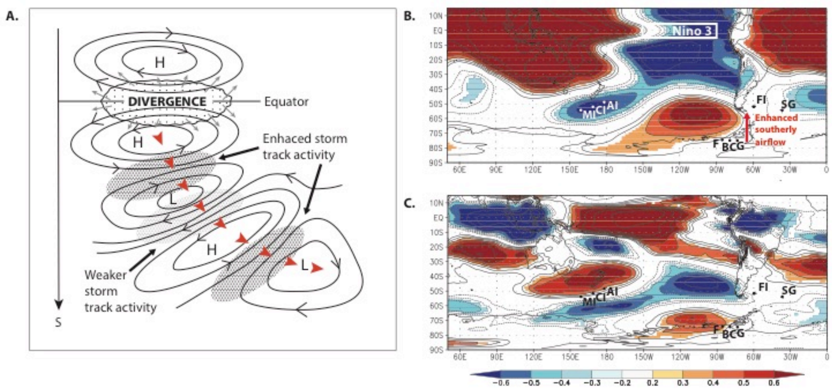

Figure 6. Rossby wave propagation from the tropical Pacific during the austral spring-summer. Low to high latitude atmospheric teleconnections during the austral spring and summer (October-March). Schematic showing extratropical Pacific-South America (PSA) Rossby wave train (red arrows) associated with low and high pressure systems generated by anomalous equatorial upper-level divergence flow (Trenberth et al., 1998); enhanced southerly airflow across the West Antarctic coastline extends into the South Atlantic during anomalously high temperatures in the Nino 3 region (**A.**). Spatial correlations between detrended and deseasonalised Nino 3 sea surface temperature (Rayner et al., 2003) (October-March) and 850 hPa height (**B.**) and zonal wind stress (**C.**) using ERA Interim (Dee et al., 2011) for the period 1979-2015. Location of key sites are shown. Significance $p_{field} < 0.05$.

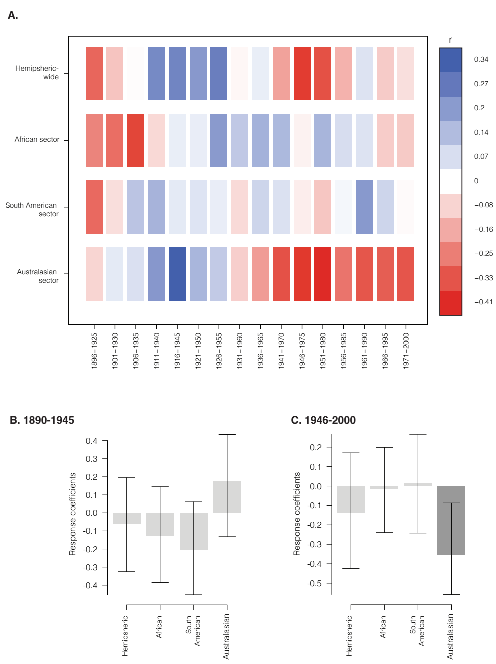

Figure 7: Changing Southern Annular Mode (SAM) relationships through the twentieth century. Running 30-year correlations (**A.**) and bootstrap correlations (**B.** and **C.**) between hemispheric-wide and sector-specific SAM reconstructions (July-October) (Visbeck, 2009) and the *Dracophyllum* series. Bootstrap correlation periods obtained by halving the SAM dataset spanning 1890 to 2000. The dark bar indicates only the Australasian SAM has a statistically significant correlation to the temperature-sensitive tree-ring series during the post-1940s period for the austral winter and early spring ($p < 0.05$).

© Author(s) 2016. CC-BY 3.0 License.

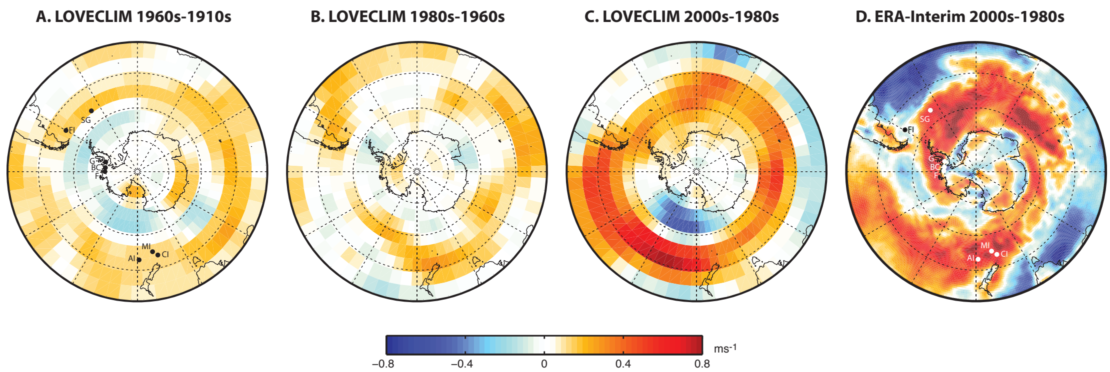

558

559 **Figure 8. Modelled changes in Southern Hemisphere westerly airflow over the last century.** Differences in zonal October-March wind speed (ms^{-1}) at 800 hPa across the Southern Oce
560 derived from LOVECLIM1.3 (Zunz and Goosse, 2015) (Panels A.-C.) and ERA-Interim (Dee et al., 2011) (Panel D.). Location of key sites discussed in text are also shown.

© Author(s) 2016. CC-BY 3.0 License.

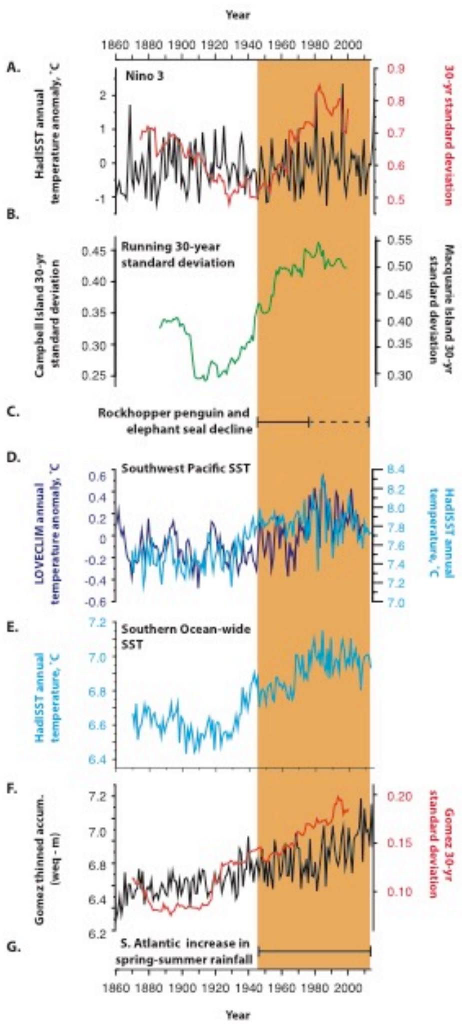

Figure 9. Equatorial and south Pacific temperature and marine population trends since CE 1860. Nino 3 temperature (July-June) with running 30-year mean standard deviation of the HadISST temperature series (Rayner et al., 2003) (**A.**) compared against Campbell Island and Macquarie Island running 30-year mean standard deviation of the reconstructed temperature series (**B.**). Orange column denotes twentieth century temperature variability that exceeds any other period in the record. Onset (solid line) and continuing (dashed) period of declining rockhopper penguin and elephant seal populations in the southwest Pacific (Morrison et al., 2015; Weimerskirch et al., 2003) (**C.**) shown for comparison. In addition, mean annual temperature (°C, July-June) sea surface temperatures (HadISST and LOVECLIM model output) for the Campbell-Macquarie islands region (**D.**) and wider Southern Ocean (**E.**). Note the coincident increase in west Antarctic coast (Gomez) (annual and 30-year mean standard deviation) (Thomas et al., 2015; Thomas et al., 2008) (**G.**) and south Atlantic (Falkland Islands and South Georgia) precipitation (Turney et al., 2016) (**F.**).

Clim. Past Discuss., doi:10.5194/cp-2016-114, 2016
Manuscript under review for journal Clim. Past
Published: 21 November 2016
© Author(s) 2016. CC-BY 3.0 License.

	Nino 4	Nino 3.4	Nino 3	Nino 1+2	SOI
Macquarie Is					
July-June	-0.392*	-0.512†	**-0.563‡**	**-0.558‡**	0.470†
October-March	-0.396*	-0.523†	**-0.596‡**	**-0.614‡**	0.475†
Campbell Is					
July-June	-0.412*	-0.514†	**-0.546‡**	-0.531†	0.458†
October-March	-0.409*	-0.534†	**-0.592‡**	**-0.582‡**	0.473†

Table 1: Correlations and significance of relationship between subantarctic island air temperatures and measures of equatorial Pacific sea surface temperature (SST) and atmospheric circulation. Nino region temperature anomalies as calculated from HadISST(Rayner et al., 2003); the Southern Oscillation Index (SOI) as reported by Ropelewski and Jones (1987). Deseasonalised and detrended correlations derived for the period CE 1979 to 2014. Significance indicated as follows: *p<0.05, † p<0.01, and ‡ p<0.001.

References

Abram, N. J., Mulvaney, R., Vimeux, F., Phipps, S. J., Turner, J., and England, M. H.: Evolution of the Southern Annular Mode during the past millennium, Nature Climate Change, 4, 564-569, 2014.
Adamson, D. A., Whetton, P., and Selkirk, P. M.: An analysis of air temperature records for Macquarie Island: decadal warming, ENSO cooling and Southern Hemisphere circulation patterns, Papers and Proceedings of the Royal Society of Tasmania, 122, 107-112, 1988.
Biondi, F. and Waikul, K.: DENDROCLIM2002: A C++ program for statistical calibration of climate signals in tree-ring chronologies, Computers and Geosciences, 30, 303–311, 2003.
Boersma, P. D. and Rebstock, G. A.: Climate change increases reproductive failure in Magellanic penguins, PLoS ONE, 9, e85602, 2014.
Boyd, P. W., Lennartz, S. T., Glover, D. M., and Doney, S. C.: Biological ramifications of climate-change-mediated oceanic multi-stressors, Nature Climate Change, 5, 71-79, 2015.
Brohan, P., Kennedy, J. J., Harris, I., Tett, S. F. B., and Jones, P. D.: Uncertainty estimates in regional and global observed temperature changes: A new data set from 1850, Journal of Geophysical Research, 111, D12106, 2006.
Brovkin, V., Bendtsen, J., Claussen, M., Ganopolski, A., Kubatzki, C., Petoukhov, V., and Andreev, A.: Carbon cycle, vegetation, and climate dynamics in the Holocene: Experiments with the CLIMBER-2 model, Global Biogeochemical Cycles, 16, 86-81-86-20, 2002.
Chelton, D. B. and Risien, C. M.: Zonal and meridional discontinuities and other issues with the HadISST1.1 dataset, Oregon State University, Corvallis, Oregon, 18 pp., 2016.
Ciasto, L. M. and Thompson, D. W. J.: Observations of large-scale ocean–atmosphere interaction in the Southern Hemisphere, Journal of Climate, 21, 1244-1259, 2008.
Cobb, K. M., Westphal, N., Sayani, H. R., Watson, J. T., Di Lorenzo, E., Cheng, H., Edwards, R. L., and Charles, C. D.: Highly variable El Niño-Southern Oscillation throughout the Holocene, Science, 339, 67-70, 2013.
Cook, E. R. and Kairiukstis, L. A.: Methods of Dendrochronology: Applications in the Environmental Sciences, Kluwer Academic Publishers, Dordrecht, Netherlands, 1990.
Cook, E. R. and Peters, K.: Calculating unbiased tree-ring indices for the study of climatic and environmental change, The Holocene, 7, 361-370, 1997.
Cunningham, D. and Moors, P.: The decline of Rockhopper penguins *Eudyptes chrysocome* at Campbell Island, Southern Ocean and the influence of rising sea temperatures, Emu, 94, 27-36, 1994.
Dee, D. P., Uppala, S. M., Simmons, A. J., Berrisford, P., Poli, P., Kobayashi, S., Andrae, U., Balmaseda, M. A., Balsamo, G., Bauer, P., Bechtold, P., Beljaars, A. C. M., van de Berg, L., Bidlot, J., Bormann, N., Delsol, C., Dragani, R., Fuentes, M., Geer, A. J., Haimberger, L., Healy, S. B., Hersbach, H., Hólm, E. V., Isaksen, L., Kållberg, P., Köhler, M., Matricardi, M., McNally, A. P., Monge-Sanz, B. M., Morcrette, J. J., Park, B. K., Peubey, C., de Rosnay, P., Tavolato, C., Thépaut, J. N., and Vitart, F.: The ERA-Interim reanalysis: configuration and performance of the data assimilation system, Quarterly Journal of the Royal Meteorological Society, 137, 553-597, 2011.
Ding, Q., Steig, E. J., Battisti, D. S., and Wallace, J. M.: Influence of the tropics on the Southern Annular Mode, Journal of Climate, 25, 6330-6348, 2012.

© Author(s) 2016. CC-BY 3.0 License.

Dubinkina, S. and Goosse, H.: An assessment of particle filtering methods and nudging for climate state reconstructions, Climate of the Past, 9, 1141-1152, 2013.

Fogt, R. L., Jones, J. M., and Renwick, J.: Seasonal zonal asymmetries in the Southern Annular Mode and their impact on regional temperature anomalies, Journal of Climate, 25, 6253-6270, 2012.

Freitas, A. C., Frederiksen, J. S., Whelan, J., O'Kane, T. J., and Ambrizzi, T.: Observed and simulated inter-decadal changes in the structure of Southern Hemisphere large-scale circulation, Climate Dynamics, 45, 2993-3017, 2015.

Friedman, J. H.: A Variable Span Smoother, Laboratory for Computational Statistics, Department of Statistics, Stanford University 1984.

Goosse, H., Brovkin, V., Fichefet, T., Haarsma, R., Huybrechts, P., Jongma, J., Mouchet, A., Selten, F., Barriat, P.-Y., and Campin, J.-M.: Description of the Earth system model of intermediate complexity LOVECLIM version 1.2, Geoscientific Model Development, 3, 603-633, 2010.

Goosse, H. and Fichefet, T.: Importance of ice-ocean interactions for the global ocean circulation: A model study, Journal of Geophysical Research, 104, 23337-23355, 1999.

Goosse, H. and Renssen, H.: A simulated reduction in Antarctic sea-ice area since 1750: implications of the long memory of the ocean, International Journal of Climatology, 25, 569-579, 2005.

Goosse, H., Renssen, H., Timmermann, A., Bradley, R., and Mann, M.: Using paleoclimate proxy-data to select optimal realisations in an ensemble of simulations of the climate of the past millennium, Climate Dynamics, 27, 165-184, 2006.

Goosse, H. and Zunz, V.: Decadal trends in the Antarctic sea ice extent ultimately controlled by ice–ocean feedback, The Cryosphere, 8, 453-470, 2014.

Harsch, M. A., McGlone, M. S., and Wilmshurst, J.: Winter climate limits subantarctic low forest growth and establishment, PLoS ONE, doi: 10.1371/journal.pone.0093241, 2014. doi:10.1371/journal.pone.0093241, 2014.

Hiscock, J. A. and Chilvers, B. L.: Declining eastern rockhopper (*Eudyptes filholi*) and erect-crested (*E. sclateri*) penguins on the Antipodes Islands, New Zealand, New Zealand Journal of Ecology, 38, 124-131, 2014.

Hosking, J. S., Orr, A., Marshall, G. J., Turner, J., and Phillips, T.: The influence of the Amundsen–Bellingshausen Seas Low on the climate of West Antarctica and its representation in coupled climate model simulations, Journal of Climate, 26, 6633-6648, 2013.

Jones, J. M., Gille, S. T., Goosse, H., Abram, N. J., Canziani, P. O., Charman, D. J., Clem, K. R., Crosta, X., de Lavergne, C., Eisenman, I., England, M. H., Fogt, R. L., Frankcombe, L. M., Marshall, G. J., Masson-Delmotte, V., Morrison, A. K., Orsi, A. J., Raphael, M. N., Renwick, J. A., Schneider, D. P., Simpkins, G. R., Steig, E. J., Stenni, B., Swingedouw, D., and Vance, T. R.: Assessing recent trends in high-latitude Southern Hemisphere surface climate, Nature Clim. Change, 6, 917-926, 2016.

Kestin, T. S., Karoly, D. J., Yano, J.-I., and Rayner, N. A.: Time–frequency variability of ENSO and stochastic simulations, Journal of Climate, 11, 2258-2272, 1998.

Kidson, E.: Meteorology. Discussions of Observations at Adélie Land, Queen Mary Land and Macquarie Island, Sydney, 121 pp., 1946.

Langlais, C. E., Rintoul, S. R., and Zika, J. D.: Sensitivity of Antarctic Circumpolar Current transport and eddy activity to wind patterns in the Southern Ocean, Journal of Physical Oceanography, 45, 1051-1067, 2015.

Loewe, F.: A further note on the sea water temperatures at Macquarie Island, Australian Meteorological Magazine, 16, 118-119, 1968.

Loewe, F.: A note on the sea water temperatures at Macquarie Island, Australian Meteorological Magazine, 19, 60-61, 1957.

Marshall, G.: Trends in the Southern Annular Mode from observations and reanalyses, Journal of Climate, 16, 4134-4143, 2003.

Masumoto, Y., Sasaki, H., Kagimoto, T., Komori, N., Ishida, A., Sasai, Y., Miyama, T., Motoi, T., Mitsudera, H., Takahashi, K., Sakuma, H., and Yamagata, T.: A fifty-year eddy-resolving simulation of the world ocean – Preliminary outcomes of OFES (OGCM for the Earth simulator), Journal of the Earth Simulator, 1, 35-56, 2004.

McGlone, M. S., Turney, C. S. M., Wilmshurst, J. M., and Pahnke, K.: Divergent trends in land and ocean temperature in the Southern Ocean over the past 18,000 years, Nature Geoscience, 3, 622-626, 2010.

Melvin, T. M. and Briffa, K. R.: A “signal-free” approach to dendroclimatic standardisation, Dendrochronologia, 26, 71-86, 2008.

Mo, K. C. and Higgins, R. W.: The Pacific–South American modes and tropical convection during the Southern Hemisphere winter, Monthly Weather Review, 126, 1581-1596, 1998.

Morrison, K. W., Battley, P. F., Sagar, P. M., and Thompson, D. R.: Population dynamics of Eastern Rockhopper Penguins on Campbell Island in relation to sea surface temperature 1942–2012: current warming hiatus pauses a long-term decline, Polar Biology, 38, 163-177, 2015.

Newman, B. W.: Meteorology. Tabulated and Reduced Records of the Macquarie Island Station, Sydney, 539 pp., 1929.

Olive, D. J.: Prediction intervals for regression models , Computational Statistics and Data Analysis, 51, 3115-3122, 2007.

Opsteegh, J. D., Haarsma, R. J., Selten, F. M., and Kattenberg, A.: ECBILT: a dynamic alternative to mixed boundary conditions in ocean models, Tellus A, 50, 348-367, 1998.

Paris, C. B., Helgers, J., van Sebille, E., and Srinivasan, A.: Connectivity Modeling System: A probabilistic modeling tool for the multi-scale tracking of biotic and abiotic variability in the ocean, Environmental Modelling & Software, 42, 47-54, 2013.

Pritchard, H. D., Ligtenberg, S. R. M., Fricker, H. A., Vaughan, D. G., van den Broeke, M. R., and Padman, L.: Antarctic ice-sheet loss driven by basal melting of ice shelves, Nature, 484, 502-505, 2012.

© Author(s) 2016. CC-BY 3.0 License.

Qin, X., van Sebille, E., and Sen Gupta, A.: Quantification of errors induced by temporal resolution on Lagrangian particles in an eddy-resolving model, Ocean Modelling, 76, 20-30, 2014.

Rayner, N. A., Parker, D. E., Horton, E. B., Folland, C. K., Alexander, L. V., Rowell, D. P., Kent, E. C., and Kaplan, A.: Global analyses of sea surface temperature, sea ice, and night marine air temperature since the late nineteenth century, Journal of Geophysical Research: Atmospheres, 108, 4407, doi:4410.1029/2002JD002670, 2003.

Ropelewski, C. F. and Jones, P. D.: An extension of the Tahiti-Darwin Southern Oscillation Index, Monthly Weather Review, 115, 2161-2165, 1987.

Sallée, J.-B., Matear, R. J., Rintoul, S. R., and Lenton, A.: Localized subduction of anthropogenic carbon dioxide in the Southern Hemisphere oceans, Nature Geoscience, 5, 579-584, 2012.

Schneider, D. P., Okumura, Y., and Deser, C.: Observed Antarctic interannual climate variability and tropical linkages, Journal of Climate, 25, 4048-4066, 2012.

Smith, T. M. and Reynolds, R. W.: A global merged land-air-sea surface temperature reconstruction based on historical observations (1880-1997), Journal of Climate, 18, 2021-2036, 2005.

Sokolov, S. and Rintoul, S. R.: Circumpolar structure and distribution of the Antarctic Circumpolar Current fronts: 1. Mean circumpolar paths, Journal of Geophysical Research: Oceans, 114, C11018, 2009.

Steig, E. J., Schneider, D. P., Rutherford, S. D., Mann, M. E., Comiso, J. C., and Shindell, D. T.: Warming of the Antarctic ice-sheet surface since the 1957 International Geophysical Year, Nature, 457, 459-462, 2009.

Streten, N. A.: The climate of Macquarie Island and its role in atmospheric monitoring, Papers and Proceedings of the Royal Society of Tasmania, 122, 91-106, 1988.

Taylor, K. E., Stouffer, R. J., and Meehl, G. A.: An overview of CMIP5 and the experiment design, Bulletin of the American Meteorological Society, 93, 485-498, 2011.

Thomas, E. R., Hosking, J. S., Tuckwell, R. R., Warren, R., and Ludlow, E.: Twentieth century increase in snowfall in coastal West Antarctica, Geophysical Research Letters, 42, 9387-9393, 2015.

Thomas, E. R., Marshall, G. J., and McConnell, J. R.: A doubling in snow accumulation in the western Antarctic Peninsula since 1850, Geophysical Research Letters, 35, doi: 10.1029/2007GL032529, 2008.

Thompson, D. W. J., Solomon, S., Kushner, P. J., England, M. H., Grise, K. M., and Karoly, D. J.: Signatures of the Antarctic ozone hole in Southern Hemisphere surface climate change, Nature Geoscience, 4, 741-749, 2011.

Thomson, D. J.: Spectrum estimation and harmonic analysis, Proceedings of the IEEE, 70, 1055–1096, 1982.

Trathan, P. N., Forcada, J., and Murphy, E. J.: Environmental forcing and Southern Ocean marine predator populations: Effects of climate change and variability, Philosophical Transactions of the Royal Society B: Biological Sciences, 362, 2351-2365, 2007.

Trenberth, K. E., Branstator, G. W., Karoly, D., Kumar, A., Lau, N. C., and Ropelewski, C.: Progress during TOGA in understanding and modeling global teleconnections associated with tropical sea surface temperatures, Journal of Geophysical Research: Oceans, 103, 14291-14324, 1998.

Trenberth, K. E., Fasullo, J. T., Branstator, G., and Phillips, A. S.: Seasonal aspects of the recent pause in surface warming, Nature Climate Change, 4, 911-916, 2014.

Turner, J., Lu, H., White, I., King, J. C., Phillips, T., Hosking, J. S., Bracegirdle, T. J., Marshall, G. J., Mulvaney, R., and Deb, P.: Absence of 21st century warming on Antarctic Peninsula consistent with natural variability, Nature, 535, 411-415, 2016.

Turney, C. S. M., Fogwill, C. J., Klekociuk, A. R., van Ommen, T. D., Curran, M. A. J., Moy, A. D., and Palmer, J. G.: Tropical and mid-latitude forcing of continental Antarctic temperatures, The Cryosphere, 9, 2405-2415, 2015.

Turney, C. S. M., Jones, R. T., Lister, D., Jones, P., Williams, A. N., Hogg, A., Thomas, Z. A., Compo, G. P., Yin, X., Fogwill, C. J., Palmer, J., Colwell, S., Allan, R., and Visbeck, M.: Anomalous mid-twentieth century atmospheric circulation change over the South Atlantic compared to the last 6000 years, Environmental Research Letters, 11, 64009-64022, 2016.

van Sebille, E., England, M. H., Zika, J. D., and Sloyan, B. M.: Tasman leakage in a fine-resolution ocean model, Geophysical Research Letters, 39, L06601, 2012.

Visbeck, M.: A station-based Southern Annular Mode Index from 1884 to 2005, Journal of Climate, 22, 940-950, 2009.

Wang, G. and Dommenget, D.: The leading modes of decadal SST variability in the Southern Ocean in CMIP5 simulations, Climate Dynamics, 2015. doi: 10.1007/s00382-00015-02932-00383, 2015.

Wang, G., Dommenget, D., and Frauen, C.: An evaluation of the CMIP3 and CMIP5 simulations in their skill of simulating the spatial structure of SST variability, Climate Dynamics, 44, 95-114, 2015.

Wang, J., Mazloff, M. R., and Gille, S. T.: Pathways of the Agulhas waters poleward of 29°S, Journal of Geophysical Research: Oceans, doi: 10.1002/2014JC010049, 2014. doi: 10.1002/2014JC010049, 2014.

Weimerskirch, H., Inchausti, P., Guinet, C., and Barbraud, C.: Trends in bird and seal populations as indicators of a system shift in the Southern Ocean, Antarctic Science, 15, 249-256, 2003.

Wu, L., Cai, W., Zhang, L., Nakamura, H., Timmermann, A., Joyce, T., McPhaden, M. J., Alexander, M., Qiu, B., Visbeck, M., Chang, P., and Giese, B.: Enhanced warming over the global subtropical western boundary currents, Nature Climate Change, 2, 161-166, 2012.

Zang, C. and Biondi, F.: Dendroclimatic calibration in R: The bootRes package for response and correlation function analysis, Dendrochronologia, 13, 68-74, 2012.

Zunz, V. and Goosse, H.: Influence of freshwater input on the skill of decadal forecast of sea ice in the Southern Ocean, The Cryosphere, 9, 541-556, 2015.